



Provided by the author(s) and NUI Galway in accordance with publisher policies. Please cite the published version when available.

|                             |   |
|-----------------------------|---|
| Title                       | Identifications and quantitative measurements of narcotics in solid mixtures using near-IR Raman spectroscopy and multivariate analysis.  |
| Author(s)                   | Ryder, Alan G.; O Connor, Gerard M.; Glynn, Thomas J.   |
| Publication Date            | 1999  |
| Publication Information     | Alan G. Ryder, Gerard M. O Connor, and Thomas J. Glynn. (1999) 'Identifications and quantitative measurements of narcotics in solid mixtures using near-IR Raman spectroscopy and multivariate analysis'. Journal Of Forensic Sciences, 44 (5):1013-1019. |
| Publisher                   | ASTM International  |
| Link to publisher's version | <a href="http://enterprise.astm.org/DIGITAL_LIBRARY/JOURNALS/FORENSIC/PAGES/JFS12031J.htm">http://enterprise.astm.org/DIGITAL_LIBRARY/JOURNALS/FORENSIC/PAGES/JFS12031J.htm</a>   |
| Item record                 | <a href="http://hdl.handle.net/10379/3822">http://hdl.handle.net/10379/3822</a>   |

Downloaded 2023-03-23T12:07:20Z

Some rights reserved. For more information, please see the item record link above.



# Identifications and quantitative measurements of narcotics in solid mixtures using near-IR Raman spectroscopy and multivariate analysis<sup>1</sup>.

Alan G. Ryder Ph.D.\*, Gerard M. O'Connor Ph.D.\*, Thomas J. Glynn Ph.D.\*

\* National Centre for Laser Applications, Physics Department,  
National University of Ireland, Galway,  
Galway, Ireland.

Author for correspondence or reprints:

Dr. Alan G. Ryder,  
School of Chemistry,  
National University of Ireland, Galway,  
Galway,  
Ireland.

Running head line: Quantitative near-IR Raman of narcotics.

**Published Citation:** Identifications and Quantitative Measurement of Narcotics in Solid Mixtures Using Near-IR Raman Spectroscopy and Multivariate Analysis. A.G. Ryder, G.M. O'Connor, and T.J. Glynn, *Journal of Forensic Sciences*, **44**(5), 1013-1019, (1999).

**Note:** This is the final submitted version, but it may not include any proofing corrections.

---

<sup>1</sup> This work was supported by the 'Science & Technology Against Drugs' Programme of Forbairt, the National Science and Technology Agency of Ireland.

## **Abstract:**

Raman spectroscopy offers the potential for the identification of illegal narcotics in seconds by inelastic scattering of light from molecular vibrations. In this study cocaine, heroin, and MDMA were analyzed using near-IR (785 nm excitation) micro-Raman spectroscopy. Narcotics were dispersed in solid dilutants of different concentrations by weight. The dilutants investigated were foodstuffs (flour, baby milk formula), sugars (glucose, lactose, maltose, mannitol), and inorganic materials (Talc powder,  $\text{NaHCO}_3$ ,  $\text{MgSO}_4 \cdot 7\text{H}_2\text{O}$ ). In most cases it was possible to detect the presence of drugs at levels down to ~10% by weight. The detection sensitivity of the Raman technique was found to be dependent on a number of factors such as the scattering cross-sections of drug and dilutant, fluorescence of matrix or drug, complexity of dilutant Raman spectrum, and spectrometer resolution.

Raman spectra from a series of 20 mixtures of cocaine and glucose (0-100 % by weight cocaine) were collected and analyzed using multivariate analysis methods. An accurate prediction model was generated using a Partial Least Squares (PLS) algorithm that can predict the concentration of cocaine in solid glucose from a single Raman spectrum with a root mean standard error of prediction of 2.3 %.

**Key words:** Forensic Science; Raman; Spectroscopy; near-infrared; Substance abuse detection; Quantitative; multivariate analysis.

## **Introduction:**

Raman spectroscopy is based on the inelastic scattering of monochromatic light from a material. When a material is illuminated with monochromatic light, most of the light is elastically scattered (Rayleigh scattering) at the same wavelength as the incident light. The interaction of light with vibrational / rotational motion of molecules causes a very small proportion of the incident light to be inelastically scattered (Raman scattered) at different wavelengths to that of the incident light. The vibrational spectrum obtained from Raman spectroscopy is complementary to that obtained from IR spectroscopy, because of different

selection rules. IR absorption spectroscopy is based on changes in the dipole moment during molecular vibrations, whereas Raman spectroscopy involves a change in the polarizability (1). Because the Raman spectrum depends on the chemical structure of a molecule, the Raman spectrum of a molecule is unique, and, therefore, can be used as a molecular fingerprint for identification purposes as is the case with IR absorption spectroscopy.

Raman spectroscopy has a number of distinct advantages over IR absorption spectroscopy. Sample preparation in many cases is not required, permitting analysis of bulk or microscopic materials in-situ (2). Raman analysis of complex materials such as human tissue is also possible without sample pretreatment (3, 4). Unlike IR, water has a very weak Raman signal and so Raman spectra can be easily collected from aqueous solutions or moist materials (5). Raman spectroscopy generally operates from the UV to the near-IR region of the spectrum which allows for the use of fibre optic probes and compact spectrometers for remote analysis (6). Micro-Raman spectroscopy can achieve a spatial resolution approaching 1  $\mu\text{m}$  as opposed to 10-20  $\mu\text{m}$  for IR absorption spectroscopy. This high spatial resolution has allowed the Raman analysis of discrete micron-sized particles, including the determination of drug levels in individual cells (7, 8). Analysis of polymer thin films and single fibers has also been carried out both for the discrimination of materials and to probe the stereochemistry of polymers (9, 10). Increasingly, Raman spectroscopy is being used to study the chemistry and structure of complex biological polymers like proteins (11).

Specific applications of Raman spectroscopy to forensic science have been reviewed by Kuptsov (12), and several groups have employed Raman microscopy or fiber optic probes for the analysis and identification of explosive materials (13, 14, 15, 16, 17, 18). The identification of illegal drugs when dispersed through solid mixtures has been investigated by various groups who have demonstrated the possibility of using near-IR FT-Raman or UV-resonance Raman spectroscopy for narcotic identification (5, 19). Illegal drugs are generally mixed with a variety of materials that may contain contaminants, all of which may fluoresce under visible light excitation. The use of near-IR or UV excitation is required to eliminate or reduce this interference (20, 21).

Quantitative analysis using Raman spectroscopy has not yet gained wide acceptance, primarily because of difficulties associated with the complexity of light scattering from materials. Poor reproducibility of spectral intensities, problems with high signal/noise ratios and the presence of variable fluorescence have all limited the use of the technique in the past (22). However, improvements in instrumentation, and the use of multivariate analysis

techniques (Chemometrics) have been exploited to overcome these impediments. Multivariate analysis methods are used to correlate (statistically) observed spectral changes with properties such as concentration and have permitted the quantitative analysis of various complex materials (23, 24, 25, 26, 27) by Raman spectroscopy.

This paper demonstrates that a dispersive near-IR Raman spectroscopic analysis can be used for the identification of narcotic materials present in solid mixtures, a brief account of which has already been presented (28). In this work, we report for the first time an example of how Raman spectroscopy and multivariate analysis can be combined to estimate the concentration of cocaine dispersed in glucose. We also discuss a possible application of this quantitative Raman method in forensic science.

## Methods:

**1. Instrumentation:** For near-IR Raman spectroscopy the excitation source was a Ti:Sapphire solid state laser (Spectra Physics 3900s), tuned to emit at 785 nm and optically pumped using an Argon ion laser (Spectra Physics 2017). A 785 nm narrow-band interference filter was used to remove non-resonant emissions. The microscope is a modified metallurgical microscope (Nikon Optiphot) using x20 and x10 power objectives to focus the laser light on the sample, with spot sizes of  $\sim 10 \mu\text{m}$  and  $20\mu\text{m}$  respectively. The incident power at the sample was 3-8 mW. A holographic filter (HSNF-785 Kaiser Optical Inc.) was used to attenuate the elastically scattered laser light. The light was dispersed using a 0.5 m grating spectrometer (SPEX 500M) onto a liquid nitrogen cooled 512 x 512 pixel back-illuminated CCD detector (Princeton Instruments) operating at  $-120^\circ\text{C}$ . A spectral range of  $\sim 650 \text{ cm}^{-1}$  was obtained with the spectrometer operating in first order. With the entrance slit width set at  $80 \mu\text{m}$ , accumulation times varied from 30 to 800 seconds, depending on the instrument alignment and to a lesser degree the sample. For visible Raman spectroscopy at 488 and 514.5 nm, excitation was provided by the same Ar-ion laser and the Raman spectra were recorded on the same instrumental setup with separate holographic notch and interference filters. A fiber-coupled Raman Spectrometer (Holoprobe 633 Kaiser Optical Systems, Inc.), was used to acquire Raman spectra using 632.8 nm laser excitation. This spectrometer allowed collection of spectra from 100 to  $4000 \text{ cm}^{-1}$  in a single exposure ( $4 \text{ cm}^{-1}$  resolution).

**2. Materials:** MDMA hydrochloride ((±)3,4-Methylenedioxymethamphetamine-hydrochloride) and cocaine hydrochloride were supplied by Sigma-Aldrich company limited, United Kingdom, and the heroin hydrochloride was obtained from MacFarlan Smith Ltd., Edinburgh, Scotland. The dilutant materials anhydrous D-glucose (BDH), mannitol (BDH), maltose (Aldrich), and lactose (Aldrich), talc powder, NaHCO<sub>3</sub>, and MgSO<sub>4</sub>·7H<sub>2</sub>O were reagent grade. The flour used was milled wheat flour, and the baby formula was a standard commercial preparation. All materials were used as received.

Sample mixtures (5-20 mg in weight) were made up by mixing known weights of drug and dilutant, followed by grinding in an agate mortar and pestle to ensure sample homogeneity by thorough mixing of components. The mixtures were transferred to clean stainless steel hexagonal sample holders with an internal diameter of ~ 2 mm and tamped into place. Compacted mixtures produced better Raman spectra (higher signal to noise ratios) than those obtained from loose powders, as a result of maximizing the amount of material within the sampling volume. The samples for quantitative analysis were treated in the same manner.

**3. Quantitative analysis:** All spectra for quantitative analysis were collected using a single 120 second exposure under identical instrument conditions. Features in the spectra caused by cosmic rays incident on the detector were filtered out using the EasyPlot software package (ver. 3.00-7, Spiral Software+MIT). The spectra were uncorrected for instrument and detector responses. Quantitative analysis was performed using Unscrambler (V6.11a, CAMO, Trondheim, Norway) Multivariate analysis software. The spectral range was restricted to 450-1100 cm<sup>-1</sup> (510 data points) for the quantitative studies because of limitations in the equipment used. This region of the Raman spectrum was selected because of the number of strong distinct cocaine Raman bands present. All calculations were performed on a Pentium 200 MHz, 32 Mbyte RAM personal computer.

## **Results and Discussion:**

### **Qualitative analysis:**

The fluorescence behavior of the test mixtures and pure drugs was examined by recording Raman spectra at several excitation wavelengths. Table 1 illustrates the advantages

Page 5 of 19: Identifications and Quantitative Measurement of Narcotics in Solid Mixtures Using Near-IR Raman Spectroscopy and Multivariate Analysis. A.G. Ryder, G.M. O'Connor, and T.J. Glynn, *Journal of Forensic Sciences*, **44**(5), 1013-1019, (1999).

of using 785 nm as opposed to visible or 633 nm excitation sources as nearly all mixed samples fluoresced with either 488 or 514.5 nm excitation, making identification and classification of Raman bands impossible. Pure MDMA hydrochloride and heroin hydrochloride fluoresced strongly when illuminated by 488 or 514.5 nm visible light sources. The three drugs (cocaine, heroin and MDMA hydrochlorides) were investigated as the minor components (10-30% by weight) of solid mixtures. The dilutants used included lactose, glucose, maltose, mannitol, flour, baby formula, and inorganic materials. The dramatic reduction in fluorescence obtained when using 785 nm excitation to acquire the Raman spectra of MDMA dispersed in solid lactose is illustrated in figure 1. Although the use of 633 nm excitation dramatically reduced the degree of fluorescence in the solid mixtures, there was sufficient interference to render identification difficult in many cases, as illustrated in figure 2.

In this study, the determination of drug presence in a mixture was achieved by comparison of a reference spectrum of the pure drug and dilutant with that of the mixture. The degree of identification is dependent on the number of peaks that can be ascribed to the drug from the mixture spectrum. In practice this would be carried out using spectral searching and matching software in conjunction with searchable digital Raman spectral databases (5), as with IR spectroscopy.

In figures 1 and 2, Raman bands due to narcotics can easily be identified and positive identifications made when the dilutants are crystalline organic or inorganic materials. However, when a more complex and amorphous material like flour is used, the selectivity is reduced. Figure 3 shows a partial spectrum of cocaine dispersed in flour, and only the distinctive  $1599\text{ cm}^{-1}$  benzyl ring and  $1713\text{ cm}^{-1}$  carbonyl bands of cocaine are visible. In such cases Raman can only serve as a partial indicator to the presence of narcotics and additional testing is necessary for confirmation. However, Raman can be used to discriminate adulterated from non adulterated materials even when only one or two bands are visible. Digital searches of Raman spectral databases will provide best guesses and probability values as to the identity of the adulterant. Raman bands from heroin and MDMA hydrochloride could also be identified from wheat flour mixtures at the same concentration level. Identification of narcotics dispersed in other complex foodstuffs such as baby milk formula was also possible with concentrations of ~10% or greater by weight. Heroin was identified when dispersed in solid mixtures as illustrated in figure 4. As with the other two drugs, identification is possible down to ~10% for the selection of dilutants surveyed.

We have found that a number of factors can limit the sensitivity of Raman spectroscopy for the detection of specific narcotics in solid mixtures. The presence of fluorescent components has the most detrimental effect on sensitivity. However, in this study only one material (talc powder) fluoresced with 785 nm excitation. Only in this case was it impossible to identify the Raman spectrum of narcotics when dispersed in talc at drug concentrations of 10-30%. The resolution of the spectrometer or spectrograph will determine how readily one can discriminate individual narcotic and dilutant peaks that occur in the same Raman shift region. The scattering cross section of the target drug determines the strength of the Raman signal and identification will clearly become easier with stronger signals. We have observed that the intensity of the Raman spectra of the three drugs (as supplied) studied takes the following order: cocaine > heroin > MDMA. Conversely, if the dilutant(s) and contaminants have large scattering cross sections, then their Raman spectra will tend to obscure that of the narcotic. As a rule, the more complex the Raman spectrum of the dilutant the more difficult positive identification becomes, due to co-incident peaks in the spectra. The morphology and crystallinity of the bulk material can also affect the quality of Raman spectrum and, in some cases, longer exposure times may be required to obtain suitable spectra for identification purposes.

## **Quantitative analysis:**

The sample set employed (Table 2) covered a 0-100 % by weight concentration range of cocaine in order to evaluate the suitability of the method as a rapid initial screening procedure for narcotic identification. The quantitative analysis method comprises three stages: data pretreatment; data evaluation by Principal Component Analysis (PCA); and the development of calibration models for the prediction of cocaine concentration.

The Raman spectra of the samples exhibit a certain degree of variation caused by small differences in spectral collection efficiency and changes in surface composition over the sample set. This lack of consistency in the scattering (background) intensity of Raman spectra must be accounted for by pretreatment of the data before applying multivariate analysis (23). Pretreatment consisted of smoothing over an average 5 spectral data point range before performing Multiplicative Scatter Correction (MSC) for common offset to correct for baseline variation. Figure 5 depicts the changes in spectra (after pretreatment) as cocaine



concentration changes. Aspects of data pretreatment have been previously investigated (23, 26).

Principal Component Analysis (PCA) was carried out to establish what principal components (PC) or factors are responsible for the change in Raman spectra as the cocaine concentration varies. PCA on the sample set indicated that 96% of the variation in spectral data (explained X-variance) for the series of mixtures can be accounted for by three principal components. This is graphically illustrated in figure 6. The first component, PC1, accounts for 88% of the X-variance and in the graph the positive features correspond to the Raman bands of cocaine and the negative features to those of glucose. In effect, this shows that 88% of all spectral variations (for all samples) are caused by changes in cocaine concentration. This high value indicates that good quality prediction models are possible from the data.

The other two components are less important with respect to quantitative measurements. The second principal component, PC2 (5%), describes a systematic baseline variation across the spectrum from low to high wavenumber as cocaine concentration changes which is due to the changes in sample morphology as concentration of cocaine increases. The third principal component, PC3 (3%), describes small variations in peak positions particularly with regard to glucose bands. The glucose is less crystalline than the cocaine, and does not give a strong Raman spectrum and this may explain the higher degree of variation in the peak positions. Finally, the remaining 4 % is attributed to noise, and is disregarded in this study.

After having established by PCA the factors which describe the spectral data, quantitative models were developed using partial least-squares (PLS) regression algorithms (29). The results from the PLS models are shown in Table 3. The validation method used for all models was Full Cross Validation (FCV) on mean-centered data, the effectiveness of which has been discussed by Everall et al. (27). The first PLS model M1 (figure 7) was generated using a single component with the complete data set (table 2). The relatively high Root Mean Square Error of Prediction (RMSEP) of 4.1 % can be attributed to a number of data points, which do not fit the model very well. Samples 4, 5 and 10 represent measurement errors where there was a variation in surface morphology and /or the sample volume. Sample 20 (100 % glucose) is an outlier because some glucose bands overlap weak cocaine bands, thus generating a false contribution to the prediction model. Recalculation of the PLS model M1 without sample 20 results in a drop in the RMSEP to 3.7 %. Omitting these samples 4, 5, 10, 20 and recalculating produces M2 (figure 8) which was the optimum model produced in this study. Figure 9 shows the regression coefficients for M2 indicating which Raman bands

in the spectra contribute the most to the prediction of % cocaine. The low RMSEP of 2.3 % for M2 achieved the goal of the study, namely a rapid single scan Raman spectroscopic analysis from which an accurate quantitative prediction for the % cocaine in solid glucose can be obtained.

Single component models produced consistently lower RMSEP than those with two or three under similar conditions, the results are shown in table 3. The use of additional components serves only to increase the explained X-variance and the Root Mean Square Error of Correlation (RMSEC), without improving the RMSEP. This is consistent with the results from the PCA analysis, which indicates that PC's 2 and 3 account for non-concentration related changes in the spectra. Reducing the spectral range (number of data points) for PLS models, likewise, does not significantly improve the RMSEP of the prediction models.

Table 4 contains the results for prediction of % cocaine by various models on samples 7 and 17. The actual concentrations were established by proton NMR for sample 7 and by weighing for sample 17. The models produce reasonably accurate prediction results that are, however, low in both samples. The reason for the low prediction values for the two test samples is not obvious although the 9.8 % cocaine sample, being at the low end of the concentration scale, might be expected not to yield as accurate a prediction as samples near the center of the calibration set.

## Conclusions:

This study has shown that by using 785 nm excitation for Raman spectroscopy, it is possible to identify the presence of illegal drugs in a range of solid mixtures to varying degrees, depending on the type of dilutant used. This is achieved by a significant reduction in fluorescence effects using near-IR excitation. We surveyed a number of different materials and in every case identification was possible down to concentrations of ~10 % by weight. We have also shown that a dispersive near-IR Raman spectrometer can produce results equivalent to those obtained from FT-Raman but using much lower laser powers of 3-8 mW as compared to 200-500 mW (5, 19, 20). For forensic analysis, Raman spectroscopy in conjunction with searchable digital libraries of Raman spectra may best be utilised as a rapid, portable, initial screening method to ascertain the possibility of drug presence. If the presence of a drug cannot be adequately verified the technique may still be able to determine that the material

under investigation has been adulterated. Follow up analysis by GC-MS can then be used to conclusively identify the substances present for legal purposes.

We have shown that multivariate analysis methods combined with near-IR Raman spectroscopy can be used as a rapid analytical method for the analysis of narcotics in simple two component mixtures. In this case the PCA method is used to evaluate spectral data and the analysis determined that for the Raman spectra of twenty different samples, 88% of the spectral change was due only to the change in cocaine concentration. We have also shown that PLS can be used to predict the cocaine concentration in solid mixtures of cocaine dispersed in glucose with a good degree of accuracy, which should be sufficient for screening of samples. The multivariate analysis methods are rapid (1-2 minutes) and can accommodate large data sets. Improvements in the sampling method (multiple scans per sample) and instrumentation (higher optical efficiency) will reduce the instances of outliers and improve the accuracy of the quantitative models.

For practical forensic analysis of narcotic-containing material, the procedure requires that the components of the materials under investigation be known in order that the calibration models can be generated in the laboratory. As a consequence the method is not suitable for all types of seized narcotic samples. It may be suitable for materials where the composition or manufacture is well regulated or consistent such as explosives, polymer blends or tablet formulations. Further work is continuing to develop and refine the method by examining more complex three and four component mixtures.

**Table 1**

**Survey of the fluorescence behavior of drugs, dilutants and mixtures at various excitation wavelengths. F = fluorescence, N = no fluorescence.**

| <b>Drug</b>    | <b>Dilutant</b>                         | <b>Excitation Wavelength (nm)</b> |              |            |            |
|----------------|---|-----------------------------------|--------------|------------|------------|
|                |   | <b>488</b>                        | <b>514.5</b> | <b>633</b> | <b>785</b> |
| <b>Heroin</b>  | <b>none</b>                             | F                                 | F            | --         | N          |
| <b>Cocaine</b> | <b>none</b>                             | N                                 | N            | N          | N          |
| <b>MDMA</b>    | <b>none</b>                             | F                                 | F            | F          | N          |
| <b>MDMA</b>    | <b>baby milk<br/>formula</b>            | --                                | F            | F          | N          |
| <b>MDMA</b>    | <b>flour</b>                            | F                                 | F            | F          | N          |
| <b>MDMA</b>    | <b>maltose</b>                          | F                                 | F            | F          | N          |
| <b>MDMA</b>    | <b>lactose</b>                          | F                                 | F            | F          | N          |
| <b>MDMA</b>    | <b>NaHCO<sub>3</sub></b>                | F                                 | F            | F          | N          |
| <b>MDMA</b>    | <b>MgSO<sub>4</sub>.7H<sub>2</sub>O</b> | F                                 | F            | F          | N          |
| <b>MDMA</b>    | <b>mannitol</b>                         | --                                | F            | F          | N          |
| <b>Cocaine</b> | <b>maltose</b>                          | F                                 | F            | F          | N          |
| <b>Cocaine</b> | <b>NaHCO<sub>3</sub></b>                | N                                 | F            | N          | N          |
| <b>Cocaine</b> | <b>lactose</b>                          | F                                 | F            | F          | N          |
| <b>Cocaine</b> | <b>MgSO<sub>4</sub>.7H<sub>2</sub>O</b> | --                                | F            | --         | N          |
| <b>Cocaine</b> | <b>flour</b>                            | --                                | F            | F          | N          |
| <b>Cocaine</b> | <b>baby milk<br/>formula</b>            | --                                | F            | F          | N          |
| <b>-----</b>   | <b>Talc powder</b>                      | ---                               | F            | F          | F          |

**Table 2:**

Cocaine dispersed in solid glucose. Samples employed for quantitative analysis, samples 7 and 17 were used for prediction.

| sample # | %Cocaine | sample # | %Cocaine |
|----------|----------|----------|----------|
| 1        | 100.0    | 11       | 36.5     |
| 2        | 87.3     | 12       | 28.7     |
| 3        | 76.6     | 13       | 27.4     |
| 4        | 70.4     | 14       | 24.7     |
| 5        | 65.2     | 15       | 17.7     |
| 6        | 59.6     | 16       | 14.8     |
| 7        | 69.6     | 17       | 9.8      |
| 8        | 49.5     | 18       | 9.4      |
| 9        | 45.0     | 19       | 5.2      |
| 10       | 39.2     | 20       | 0.0      |

**Table 3:**

Synopsis of results from PLS regression models for predicting % cocaine in glucose. Models M1, M3, M5 and M7 have all spectra included. M2, M4, M6 and M8 models have outliers (4, 5, 10 & 20) removed. M7 / M8 are two component and M7A / M8A are three component PLS models. The correlation coefficients are given for both calibration and prediction models with the latter in brackets.

| Model | Spectral range<br>cm <sup>-1</sup> | Explained<br>X variance %, | RMSEC | RMSEP | Correlation<br>coefficients |
|-------|------------------------------------|----------------------------|-------|-------|-----------------------------|
| M 1   | 450-1100                           | 88                         | 3.5   | 4.1   | 0.992 (0.990)               |
| M 2   | 450-1100                           | 90                         | 1.7   | 2.3   | 0.998 (0.997)               |
| M 3   | 800-1040                           | 94                         | 3.5   | 4.0   | 0.992 (0.990)               |
| M 4   | 800-1040                           | 95                         | 2.0   | 2.4   | 0.998 (0.997)               |
| M 5   | 960-1040                           | 96                         | 4.0   | 4.4   | 0.990 (0.988)               |
| M 6   | 960-1040                           | 96                         | 2.1   | 2.5   | 0.997 (0.996)               |
| M 7   | 450-1100                           | --                         | 2.4   | 3.9   | 0.996 (0.991)               |
| M 7A  | 450-1100                           | --                         | 2.2   | 4.1   | 0.997 (0.990)               |
| M 8   | 450-1100                           | --                         | 1.5   | 2.8   | 0.999 (0.995)               |
| M 8A  | 450-1100                           | --                         | 1.5   | 3.0   | 0.999 (0.994)               |

**Table 4:**

Model prediction results for samples 7 & 17 (% cocaine by weight).

|           | <b>Sample 7</b>              | <b>Sample 17</b>             |
|-----------|------------------------------|------------------------------|
|           | <b>Predicted (deviation)</b> | <b>Predicted (deviation)</b> |
| <b>M1</b> | 67.8 (2.3)                   | 7.4 (2.0)                    |
| <b>M2</b> | 67.4 (1.2)                   | 7.7 (1.0)                    |
| <b>M3</b> | 67.61 (2.1)                  | 8.3 (1.9)                    |
| <b>M4</b> | 67.4 (1.2)                   | 7.5 (1.1)                    |
| <b>M5</b> | 68.0 (2.6)                   | 8.9 (1.5)                    |
| <b>M6</b> | 67.3 (1.4)                   | 8.6 (0.9)                    |
| <b>M7</b> | 67.4 (1.3)                   | 7.7 (1.1)                    |
| <b>M8</b> | 67.8 (2.3)                   | 7.4 (2.1)                    |

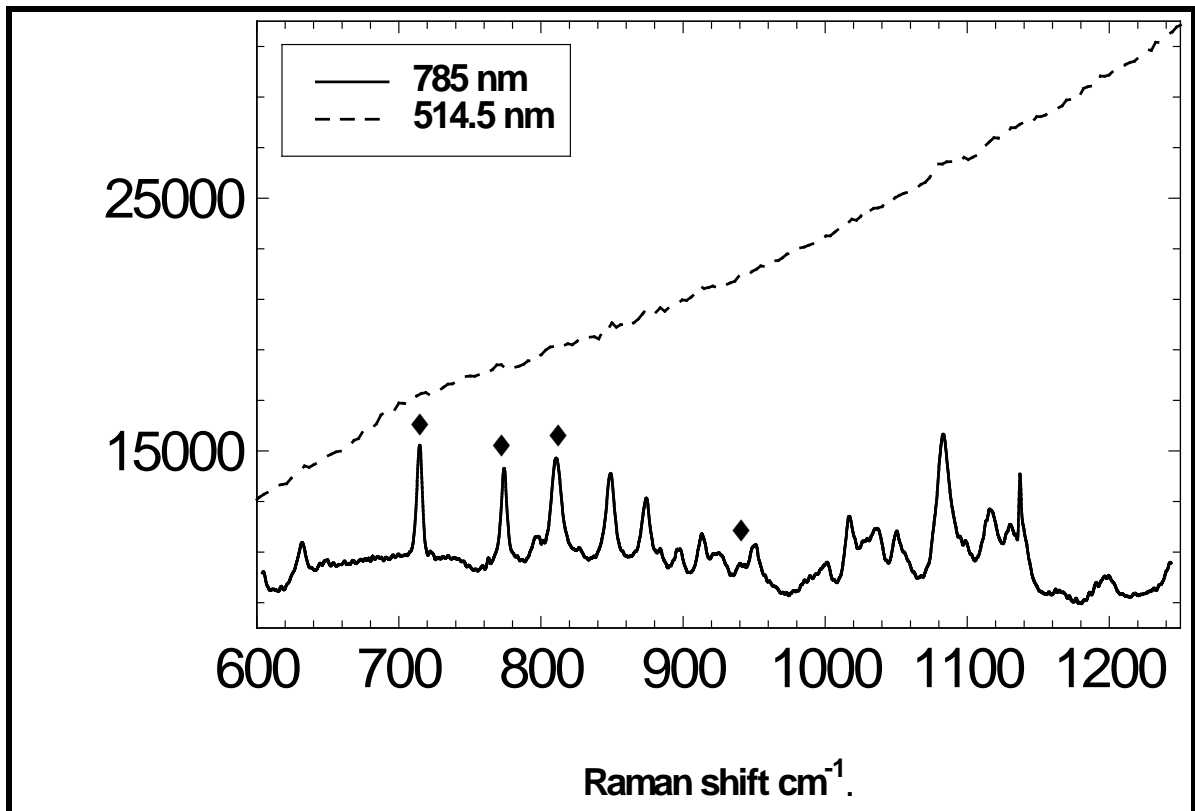


**Figure 1:** Partial Raman spectrum of 24.8% MDMA hydrochloride dispersed in lactose taken with 514.5nm excitation (dashed line), and 785nm excitation (solid). MDMA bands are marked with a ◆.

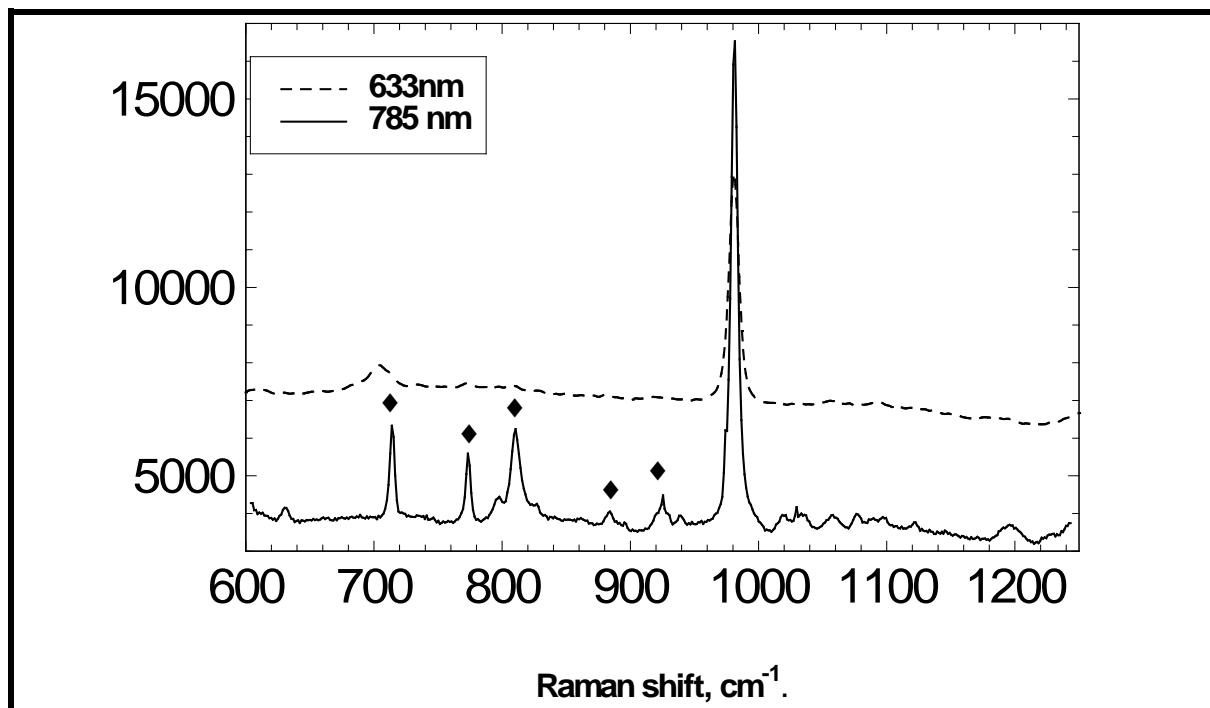


**Figure 2:** Partial Raman spectrum of MDMA hydrochloride (24%) dispersed in  $\text{MgSO}_4 \cdot 7\text{H}_2\text{O}$  taken with 633nm excitation (dashed line), and 785nm excitation (solid). MDMA bands are marked with a ♦.

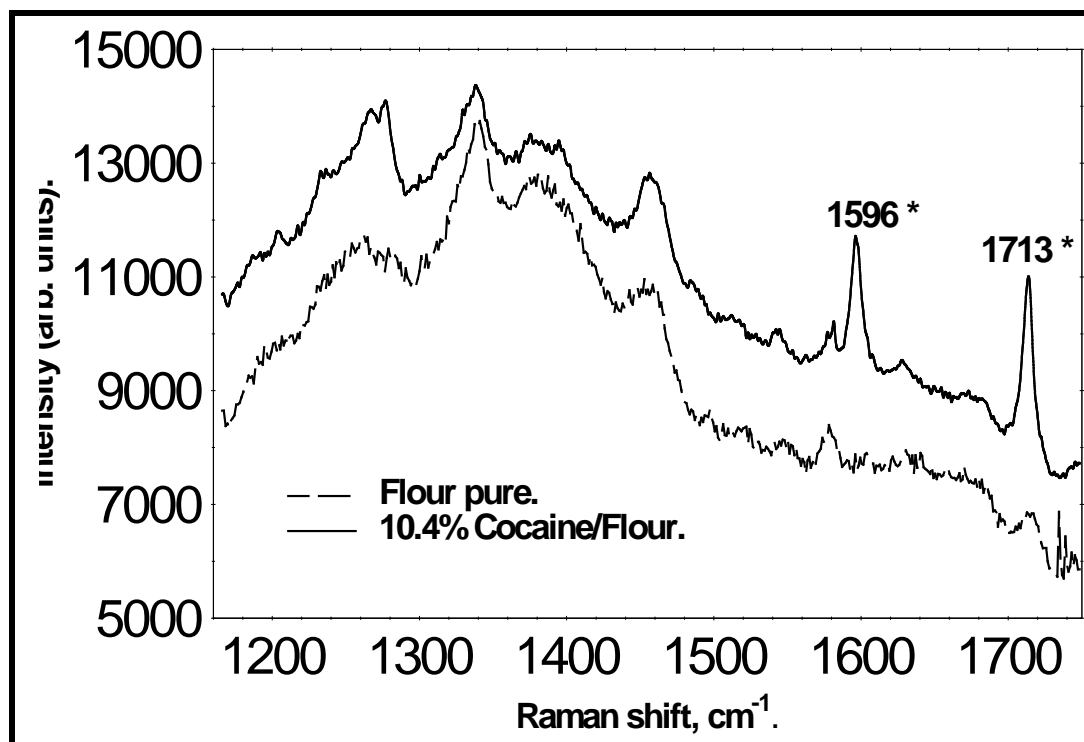


**Figure 3:** Partial Raman spectra of cocaine mixed with flour and pure flour showing cocaine phenyl ring and carbonyl bands.

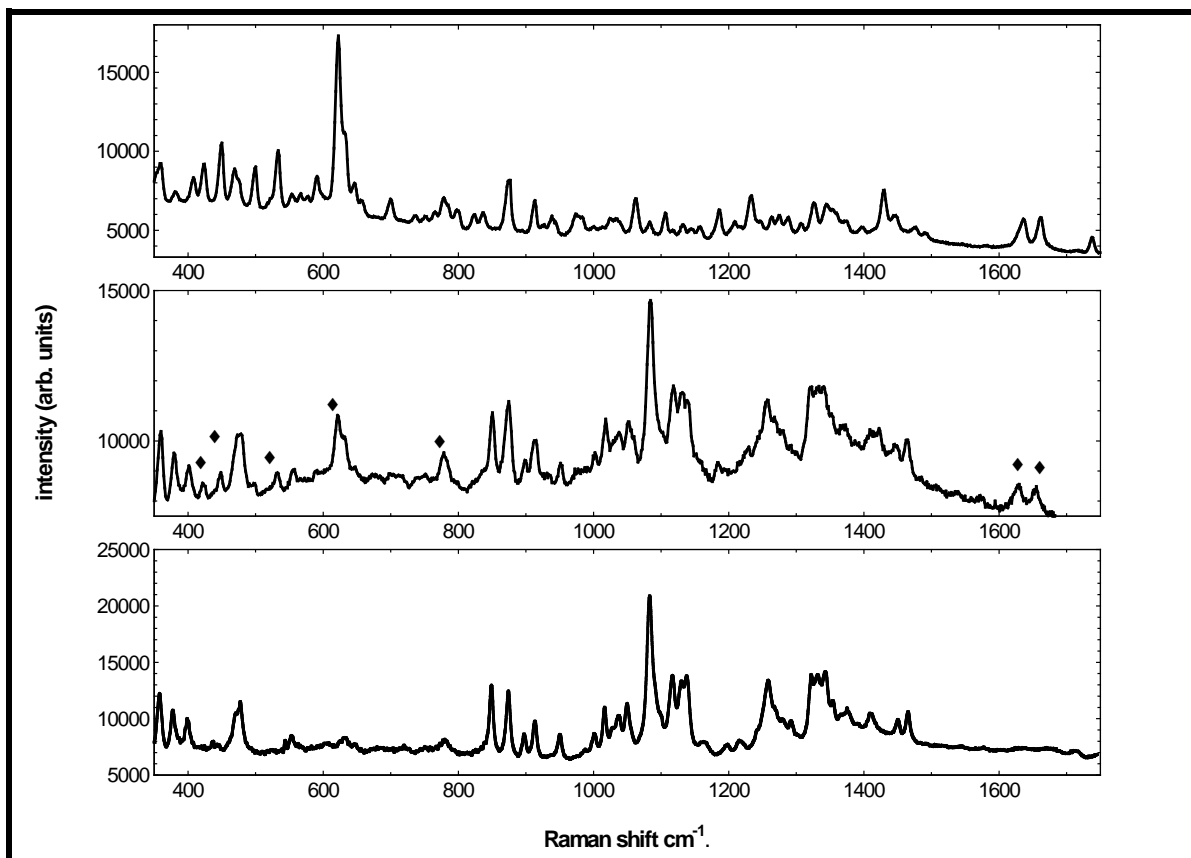


**Figure 4:** Raman spectra of heroin (top), 21% heroin/lactose (middle) and lactose (bottom) with heroin peaks marked by ♦. All spectra recorded with 785nm excitation.

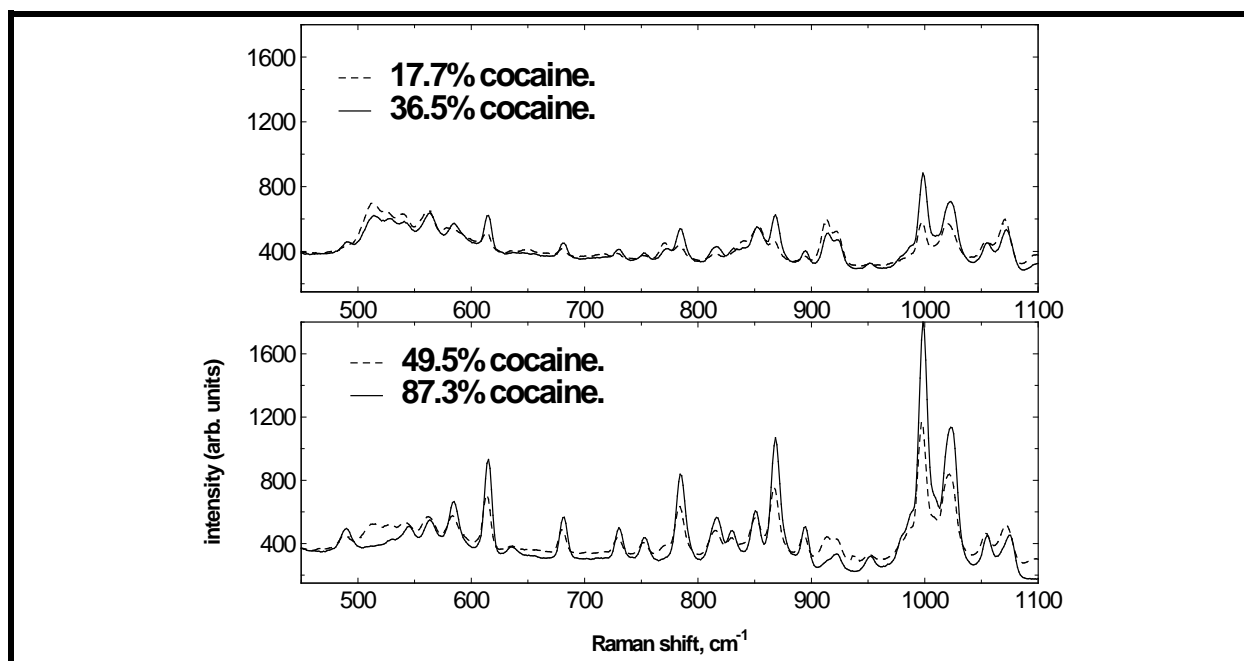


**Figure 5:** Raman spectra of cocaine and glucose mixtures using 785nm excitation. The spectra have been smoothed and the MSC common offset function applied.



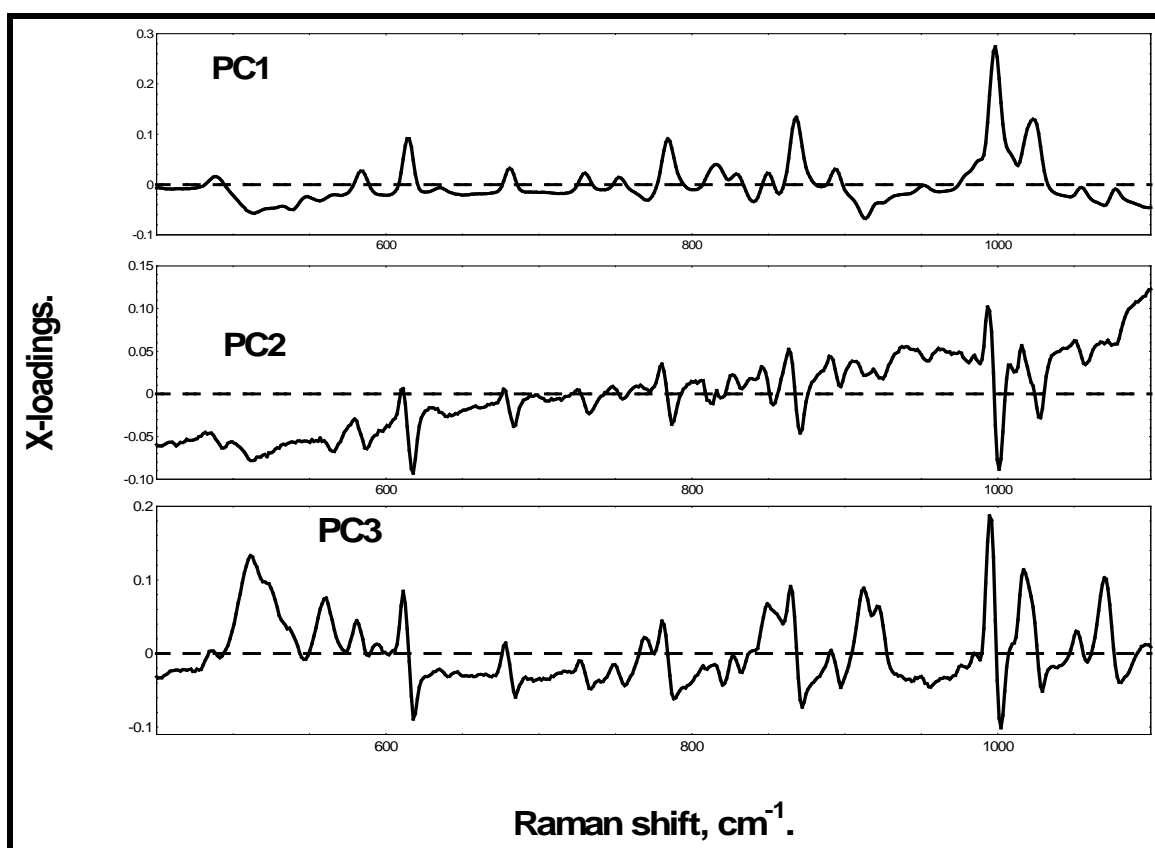


**Figure 6:** X-loading plots for the three principal components of the PCA model for the cocaine/glucose mixtures.

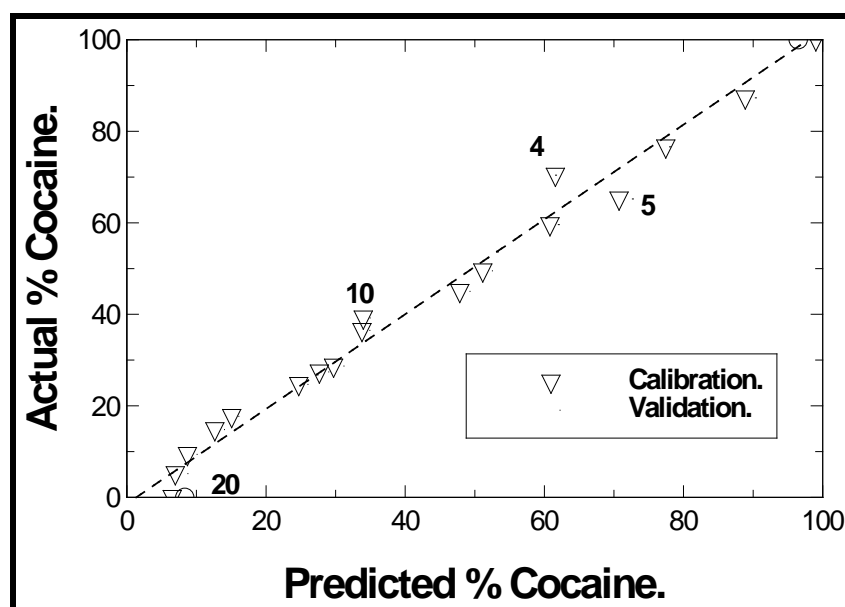


**Figure 7:** A PLS regression model (M1) for predicting the % Cocaine (by weight) dispersed in solid glucose from the Raman spectra in the 450-1100  $\text{cm}^{-1}$  range.

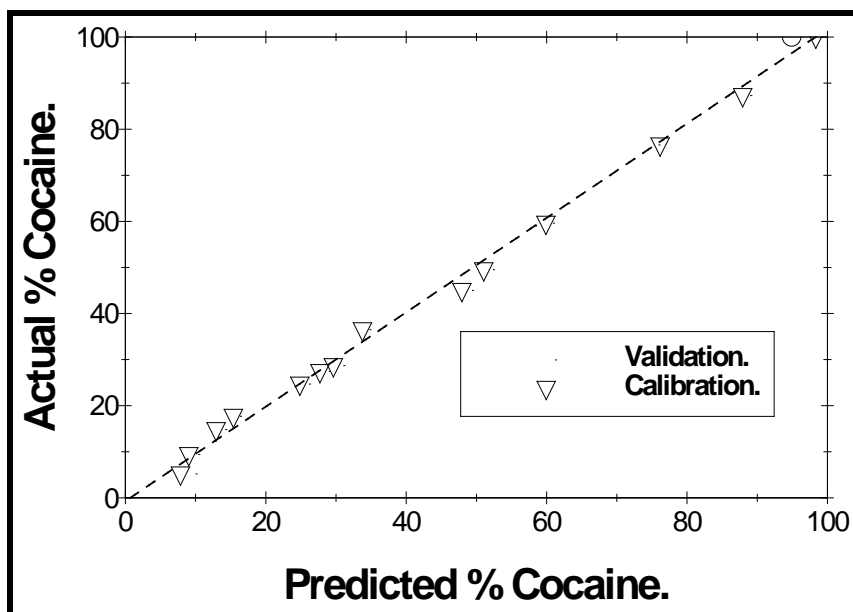


**Figure 8:** A PLS regression model (M2) for predicting the %Cocaine (by weight) dispersed in solid glucose from the Raman spectra in the 450-1100 $\text{cm}^{-1}$  range.

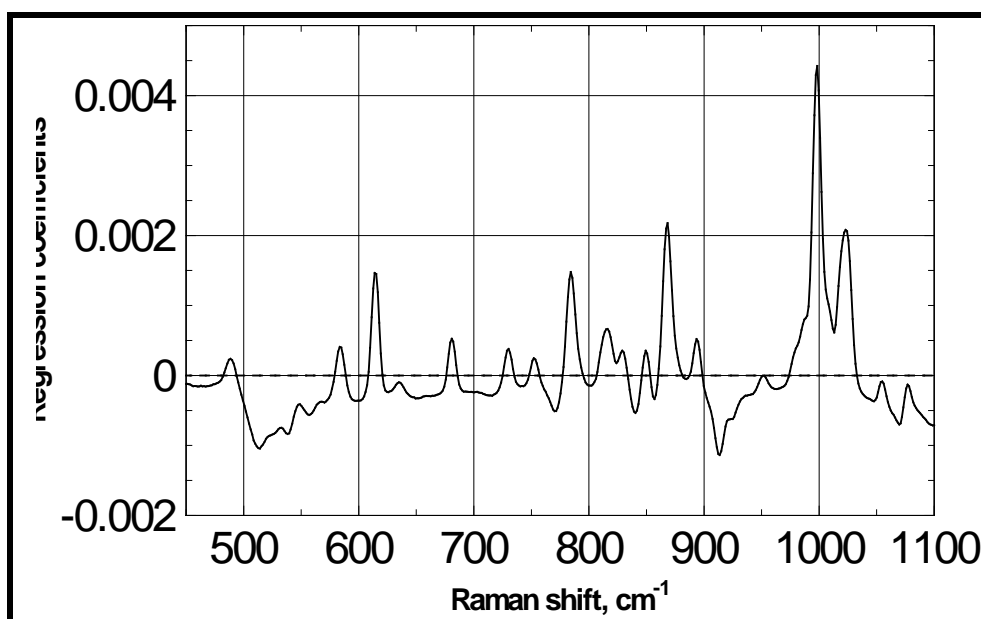


**Figure 9:** Regression coefficients for M1 prediction model.

## References:

---

- 1 Turrell G, The Raman effect: In: Turrell G, Corset J, editors. Raman microscopy: Developments and applications. London: Academic Press, 1996; 1-25.
- 2 Clark RJH, Cridland L, Kariuki BM, Harris KDM, Withnall R. Synthesis, structural characterization and Raman spectroscopy of the inorganic pigments lead tin yellow types I and II and lead antimonate yellow: Their identification on medieval paintings and manuscripts. *J Chem Soc Dalton* 1995; 2577-2582.
- 3 Lawson EE, Barry BW, Williams AC, Edwards HGM. Biomedical applications of Raman spectroscopy. *J Raman Spectrosc* 1997; 28: 111-117.
- 4 Frank CJ, Redd DCB, Gansler TS, McCreery RL. Characterization of human breast biopsy specimens with near-ir Raman spectroscopy. *Anal Chem* 1994; 66(3): 319-326.
- 5 Tsuchihashi H, Katagi M, Nishikawa M, Tatsuno M, Nishioka H, Nara A. et al. Determination of methamphetamine and its related compounds using fourier transform Raman spectroscopy. *Appl Spectrosc* 1997; 51(12): 1796-1799.
- 6 Marteau P, Adar F, Zanier-Szydowski N. Application of remote Raman measurements to the monitoring and control of chemical processes. *Am Lab* 1996; 28(16): 21H-21Q.
- 7 Freeman TL, Cope SE, Stringer MR, Cruse-Sawyer JE, Batchelder DN, Brown SB. Raman spectroscopy for the determination of photosensitizer localization in cells. *J Raman Spectrosc* 1997; 28: 641-643.
- 8 Bakker-Schut TC, Puppels GJ, Kraan YM, Greve J, van der Maas LLJ, Figdor CG. Intracellular carotenoid levels measured by Raman microspectroscopy: comparison of lymphocytes from lung cancer patients and healthy individuals. *Int J Cancer (Pred Oncol)* 1997; 74: 20-25.
- 9 Xue G. Fourier transform Raman spectroscopy and its applications for the analysis of polymeric materials. *Prog Polymer Sci* 1997; 22: 313-406.
- 10 Bouffard SP, Sommer AJ, Katon JE, Godber S. Use of molecular microspectroscopy to characterize pigment-loaded polypropylene single fibers. *Appl Spectrosc* 1994; 48(11): 1387-1393.
- 11 Carey PR. Raman spectroscopy in enzymology: the first 25 years. *J Raman Spectrosc* 1998; 29: 7-14.
- 12 Kuptsov AH. Applications of fourier transform Raman spectroscopy in forensic science. *J Forensic Sci* 1994; 39: 305-318.
- 13 Cheng C, Kirkbride TE, Batchelder DN, Lacey RJ, Sheldon TG. In situ detection and identification of trace explosives by Raman microscopy. *J Forensic Sci* 1995; 40(1): 31-37.
- 14 Hayward IP, Kirkbride TE, Batchelder DN, Lacey RJ. Use of a fibre optic probe for the detection and identification of explosive materials by Raman spectroscopy. *J Forensic Sci* 1995; 40(5): 883-884.
- 15 Lewis IR, Daniel Jr. NW, Chaffin NC, Tungol M.W. Raman spectroscopic studies of explosive materials towards a fieldable explosives detector. *Spectrochim Acta A* 1995; 51(12): 1985-2000.

- 
- 16 Daniel Jr. NW, Lewis IR, Griffiths PR. Interpretation of Raman Spectra of nitro-containing explosive materials. Part 1: Group frequency and structural class membership. *Appl Spectrosc* 1997; 51(12), 1854-1867.
  - 17 Daniel Jr. NW, Lewis IR, Griffiths PR. Interpretation of Raman spectra of nitro-containing explosive materials. Part 2: The implementation of neutral, fuzzy, and statistical models for unsupervised pattern recognition. *Appl Spectrosc* 1997; 51(12), 1868-1879.
  - 18 Fell Jr. NF, Vanderhoff JA, Pesce-Rodriguez RA, McNesby KL. Characterisation of Raman spectral changes in energetic materials and propellants during heating. *J Raman Spectrosc* 1998; 29: 165-172.
  - 19 Hendra PJ, Hodges CM, Willis HA, Farley T. Fourier transform Raman spectroscopy of illicit drugs. *J Raman Spectrosc* 1989; 20: 745-749.
  - 20 Akhavan J, Hodges CM. The use of fourier transform Raman spectroscopy in the forensic identification of illicit drugs and explosives. *Spectrochim Acta* 1990; 46A(2): 303-307.
  - 21 Sands HS, Hayward IP, Kirkbride TE, Bennett R, Lacey RJ, Batchelder DN. UV-excited resonance Raman spectroscopy of narcotics and explosives. *J Forensic Sci* 1998; 43(3): 509.
  - 22 Vickers TJ, Mann CK. Quantitative analysis by Raman spectroscopy. In: Bulkin BJ, Grasselli JG, editors. *Analytical Raman Spectroscopy*. Chemical Analysis volume 114. New York: John Wiley and Sons, Inc, 1991; 107-135.
  - 23 Shimoyama M, Maeda H, Matsukawa K, Inoue H, Nimomiya T, Ozaki Y. Discrimination of ethylene / vinyl acetate copolymers with different composition and prediction of the vinyl acetate content in the copolymers using fourier-transform Raman spectroscopy and multivariate data analysis. *Vib Spectrosc* 1997; 14: 253-259.
  - 24 Archibald DD, Kays SE, Himmelsbach DS, Barton II FE. Raman and nir spectroscopic methods for determination of total dietary fiber in cereal foods: A comparative study. *Appl Spectrosc* 1998;52(1):22-31.
  - 25 Cooper JB, Wise KL, Welch WT, Sumner MB, Wilt BK, Bledsoe RR. Comparison of near-ir, Raman and mid-ir spectroscopies for the determination of btex in petroleum fuels. *Appl Spectrosc* 1997;51(11): 1613-1620.
  - 26 Williams KPJ, Everall, NJ. Use of micro Raman spectroscopy for the quantitative determination of polyethylene density using partial least-squares calibration. *J Raman Spectrosc* 1995; 26: 427-433.
  - 27 Everall N, Chalmers JM, Ferwerda R, van der Maas JH, Hendra PJ. Measurement of poly(aryl ether ether ketone) crystallinity in isotropic and uniaxial samples using fourier transform-Raman spectroscopy: a comparison of univariate and partial least-squares calibrations. *J Raman Spectrosc* 1994; 25: 43-51.
  - 28 Ryder AG, O'Connor GM, Glynn, TJ. Near-IR Raman spectroscopy as a tool for the identification of illegal drugs in solid mixtures. In: *Proceedings of The European Union Symposium-Fighting Crime Through Technology*; 1998 Mar 24-25; London. In Press.
  - 29 Geladi P, Kowalski BR. Partial least-squares regression: a tutorial. *Anal Chim Acta* 1986; 185: 1-17.